Spectral Variation of Total Column Aerosol Optical Depth over Rajkot: A Tropical Semi-arid Indian Station

Ritweej Rajeev Ranjan, H.P. Joshi, K.N. Iyer[*]

Department of Physics, Saurashtra University, Rajkot-360005, India

Abstract

Spectral aerosol optical depth (AOD) measurements, estimated from two hand-held, microprocessor-based sun photometers [MICROTOPS-II (version 2.43 & 5.5)] over Rajkot, India were analyzed from March 2005 to March 2006 (a total of 167 days of clear-sky observations). The results showed seasonal variation with high values in summer and low values in winter. The summer increase is found to be due to the high wind speed producing larger amounts of wind-driven dust particles. The winter AOD values decrease more at higher wavelengths, indicating a general reduction in the number of bigger particles. Also during the winter months the wind direction changed to southerly and southeasterly bringing air from more rural areas to the measurement site. The amplitude of the observed high AOD values in summer is higher (low during winter) for longer wavelengths, which shows that coarse particles contribute more to the observed variation as compared to sub-micron particles. To characterize the aerosol optical depths, the Ångström parameters α and β were used.

Keywords: Atmospheric aerosol; Aerosol optical depth; Ångström parameters; Sun photometer.

* Corresponding author. Tel:+91 281-2588428, Fax: +91 281 2577633

  E-mail address: ritweej_srivastava@yahoo.co.in

INTRODUCTION

Aerosols play an important role in earth's radiation budget, air quality and environmental health (Prospero *et al.*, 1983; Satheesh and Ramanathan, 2000; Pinker *et al.*, 2001). On a global scale, the natural sources of aerosols are more important than the anthropogenic aerosols, but regionally anthropogenic aerosols are more important (Kaufman and Fraser, 1983; Ramanathan *et al.*, 2001). Aerosols produced from different natural and man-made activities are mixed together and hence each aerosol particle is a composite of different chemical constituents, which determine the refractive index of aerosols. The sources and sinks of aerosols are so varied and distributed over the globe, that their physical properties and optical effects show distinct variation with geographic locations. Natural sources, such as volcanic activity, produce synoptic scale effects; while other sources, such as wind blown dust, sea-spray, convective and general circulations produce regional-scale effects in modulating background aerosols. Added to the natural sources are the anthropogenic sources of aerosols, such as combustion, industrial activity, transport and mining that contribute to regional-scale differences in aerosol properties. Aerosols generated at one place are transported over long distances by the wind systems and they produce consequent effects at locations much farther away from the source. A good example of this is the transport of Saharan dust across the Atlantic. Hence the global studies of the aerosols properties are of great importance.

One of the most important optical properties of aerosols used in the radiative transfer calculation is the Aerosol Optical Depth (AOD). It is defined as the attenuation of direct solar radiation passing through the atmosphere by scattering (angular redistribution of energy) and absorption (conversion of energy into either heat or photochemical change) due to aerosols. Monitoring AOD at different wavelengths is useful for deriving additional information on the size distribution of particles, as well as the study of its variation with season, which in turn helps to identify the variation in the source strength of different particles emitted into atmosphere. Extensive measurements of turbidity parameters have been carried out in the past at different Indian stations using single- and three-wavelength Volz sun photometers (Mani *et al.*, 1969). These studies have considerably enriched our knowledge on the atmospheric turbidity over India and have provided some background information. Krishnamoorthy *et al.* (1988), overcoming the limitations of these measurements, conducted a study at Trivandrum (India) in 1984 using three narrow-band filters. This study revealed several aspects of aerosol extinction features and brought out the need for detailed studies by making measurements at more spectral intervals. A network of Multi-Wavelength Radiometer (MWR) stations has been set up at different locations to cover different types of environments; e.g., rural, urban, coastal, marine, arid, desert, etc. A brief review of the scientific results obtained from these stations was reported by Subbaraya *et al.* (2000). To evolve a comprehensive characterization of the spatial and temporal variation in the

physical, chemical, and radiative properties of aerosols, experiments over the Arabian Sea region under ISRO-Geosphere Biosphere Programme (ISRO-GBP), Indian Ocean Experiment (INDOEX) and Arabian Sea Monsoon Experiment (ARMEX) have recently been conducted (Satheesh *et al*., 2006). There are very few measurements of aerosol characteristics from the semi-arid, near-marine locations in India, except that from Jodhpur (Subbaraya *et al*., 2000). In this paper, we present the month-to-month variation of AOD and Ångström parameters over the semi-arid Indian station Rajkot near the Arabian Sea. These results will contribute to understanding the regional characteristics of aerosols and in helping with aerosol modeling.

SITE AND INSTRUMENTATION

Rajkot ($22^o18'$N, $70^o44'$E, 142 m above MSL) is a semi-arid suburban region near the Arabian Sea. With the availability of a modern hand-held sun photometer, investigations of the AOD can be done with much more flexibility for the selection of the wavelengths and observation sites. In this study MICROTOPS-II sun photometers (fitted with narrow-band interference filter) are used for the estimation of AOD and precipitable water vapor. The complete details of the sun photometer and measuring technique have been described by Morys *et al.* (2001). The attenuation of solar radiation by aerosol particles is strongly dependent on the size of the particle and wavelength interval considered. Therefore, investigations of the spectral variation of aerosol attenuation within the near UV, visible and near infrared regions could be very informative (Adeyewa and Balogun, 2003). We have selected wavelengths of 380, 440, 500, 675, 870 and 1020 nm for studying spectral variation of aerosol properties, and 936-nm wavelength for the precipitable water vapor study.

METHOD OF DATA ANALYSIS

Radiation measurements

Estimated value of aerosol optical depths at six different wavelengths ranging from 380 nm to 1020 nm and precipitable water vapor were collected from the MICROTOPS II sun photometer. Monthly values of relative humidity, temperature and wind velocity were downloaded from the website "www.wunderground.com". The hourly observations on the visible cloud-free days are used in the present study.

Determination of Ångström parameters

The spectral dependence of AOD is typically approximated using Ångström's formula (Ångström, 1961) derived on the premise that extinction of solar radiation by aerosols (i.e., AOD)

is a continuous function of wavelength, without selective bands or lines for scattering or absorption. Thus the formula derived empirically is given as

$$\tau(\lambda) = \beta^{\alpha} \tag{1}$$

where, $\tau(\lambda)$ is the AOD measured at wavelength $\lambda(\mu m)$, β is the turbidity coefficient (related to the total aerosol content) and α is the wavelength exponent (related to the size distribution of the scattering particles). Large values of α indicate a relatively high ratio of small to large particles. It is expected that when the aerosol particles are very small, on the order of air molecules, α should approach 4 and it should approach 0 for very large particles (Holben *et al.*, 2001; Pinker *et al.*, 2001).

For the purpose of determining α and β values by linear regression, the above equation can be further expressed in the form:

$$\ln \tau(\lambda) = \ln \beta - \alpha\lambda \tag{2}$$

Substituting the derived $\tau(\lambda)$ values in the above Eq. (2), the slope of $\ln \tau(\lambda)$ vs. $\ln \lambda$ graph provides wavelength exponent α and its intercept $\ln \beta$. For spectral analysis this method of linear fitting is the best way of obtaining the Ångström parameters (Cachorro *et al.*, 1987; Maheshkumar *et al.*, 2001).

RESULTS AND DISCUSSION

June to September are normally the rainy months of the year as the rainfall pattern at Rajkot generally follows the southwest monsoon. Except for the rainy season, the weather is dry with abundant sunshine; however cloud cover is frequently seen throughout the year. Because of this, rainy-season measurements are scarce and we could not take a significant number of observations during this period. The general statistics, i.e., the mean value and standard deviation of AOD at six different wavelengths, are given in Table 1 and that of precipitable water vapor, wavelength exponent (α) and turbidity coefficient (β) are given in Table 2.

It can be seen from the Table 1 that the mean value of AOD at all wavelengths are high during summer, prior to the monsoon. Immediately after the monsoon, the mean AOD values are the lowest. The small number of data points during these months (September, October and November) is due to the poor weather conditions, which is a constraint for reliable measurements using the instrument.

Table 1. The mean value and standard deviation of AOD at six different wavelengths.

Month Year	AOD at different wavelength						Standard deviation in AOD						No. of clear days
	380 nm	440 nm	500 nm	675 nm	870 nm	1020 nm	380 nm	440 nm	500 nm	675 nm	870 nm	1020 nm	
M-05	0.233	0.219	0.204	0.168	0.156	0.108	0.07	0.06	0.06	0.05	0.05	0.04	13
A-05	0.288	0.284	0.276	0.238	0.214	0.168	0.09	0.08	0.08	0.07	0.07	0.08	26
M-05	0.309	0.304	0.295	0.259	0.248	0.233	0.10	0.10	0.10	0.10	0.09	0.09	26
J-05	0.301	0.303	0.298	0.265	0.260	0.189	0.08	0.07	0.08	0.09	0.11	0.07	13
J-05													
A-05													
S-05	0.346	0.351	0.324	0.245	0.210	0.183	0.15	0.13	0.11	0.07	0.05	0.04	9
O-05	0.341	0.329	0.296	0.201	0.155	0.092	0.17	0.15	0.12	0.08	0.06	0.05	9
N-05	0.194	0.203	0.188	0.131	0.103	0.071	0.04	0.03	0.03	0.02	0.01	0.01	6
D-05	0.302	0.295	0.269	0.185	0.139	0.098	0.10	0.09	0.08	0.06	0.04	0.04	13
J-06	0.278	0.279	0.256	0.177	0.132	0.099	0.143	0.128	0.115	0.085	0.068	0.070	22
F-06	0.269	0.275	0.254	0.176	0.133	0.088	0.096	0.079	0.069	0.047	0.039	0.041	10
M-06	0.204	0.232	0.226	0.182	0.168	0.113	0.089	0.088	0.086	0.083	0.081	0.083	20

Spectral-temporal variations in AOD

The temporal variations in columnar AOD at different wavelengths observed on a typical clear-sky day, April 1, 2005, are shown in Fig. 1(a), which clearly indicates a systematic spectral dependence according to classical Mie scattering theory. These features can be ascribed to the abundance of fine aerosol particles of continental origin. It is also clear that AOD at these wavelengths exhibits a temporal pattern with high values in the morning and late afternoon. It may be due to rush hour and high relative humidity as shown in Fig. 2(c). Comparison between Figs. 1(a) and 2(a) and (b) reveals the influence of wind on the enhancement in AOD during pre-noon and post-noon periods. It is clear from the above figure that observations were influenced by the combined air mass of both land and ocean origin, which results in high AOD. Thus, the observed changes in AOD and wind field are consistent. It may be noted that although the wind speeds are high during the pre-noon period as compared to post-noon, the enhancement in AOD is not observed. This may be due to increase in temperature during the period (Fig. 2(d)), which might have affected the surface area of some of the aerosols present in the sensing region. Nevertheless, the effect of wind is quite evident on AOD observed during the post-noon period.

Table 2. Precipitable water vapor, wavelength exponent (α) and turbidity coefficient (β).

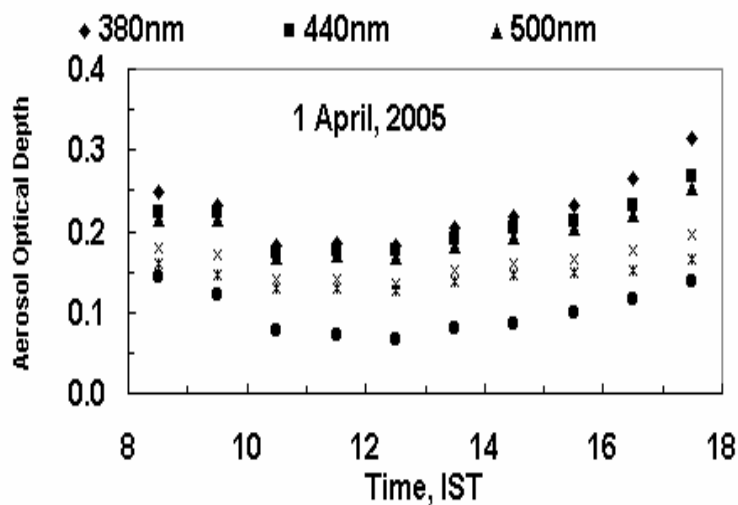| Month Year	PWC (cm)	St. Deviation	Wavelength Exponent (α)	Turbidity Coefficient (β)
M-05	1.40	0.43	0.689	0.125
A-05	1.29	0.70	0.512	0.186
M-05	2.06	0.52	0.327	0.230
J-05	3.20	0.85	0.401	0.218
J-05				
A-05				
S-05	3.78	0.89	0.699	0.189
O-05	2.47	0.53	1.277	0.113
N-05	1.13	0.06	1.036	0.083
D-05	0.97	0.34	1.147	0.112
J-06	1.04	0.29	1.083	0.110
F-06	1.46	0.23	1.135	0.104
M-06	1.30	0.48	0.584	0.136

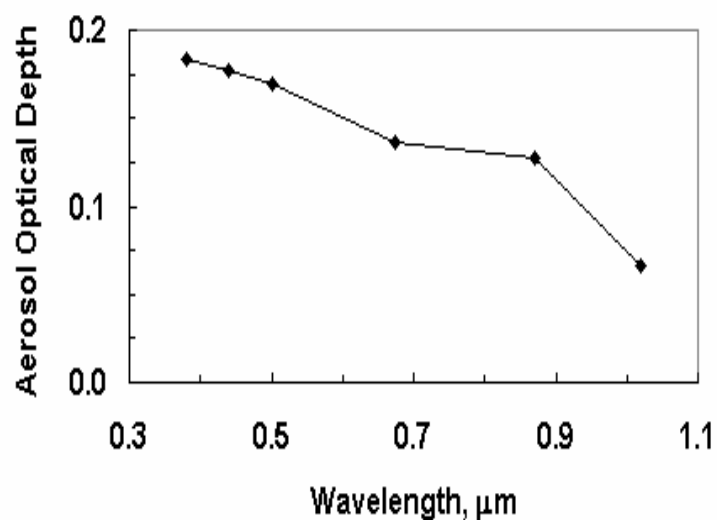**Fig. 1(a).** Temporal variations in columnar AOD at different wavelengths.

Fig. 1(b). Spectral dependence of AOD.

Fig. 1(b) shows the mean spectral dependence of AOD observed at noon time. The spectral variation of AOD exhibits high AOD at smaller wavelengths and vice-versa as expected from the Mie theory, except a slight enhancement in AOD at 870 nm, which may be due to interference of a weak water vapor-absorption band (Dani *et al.*, 2003).
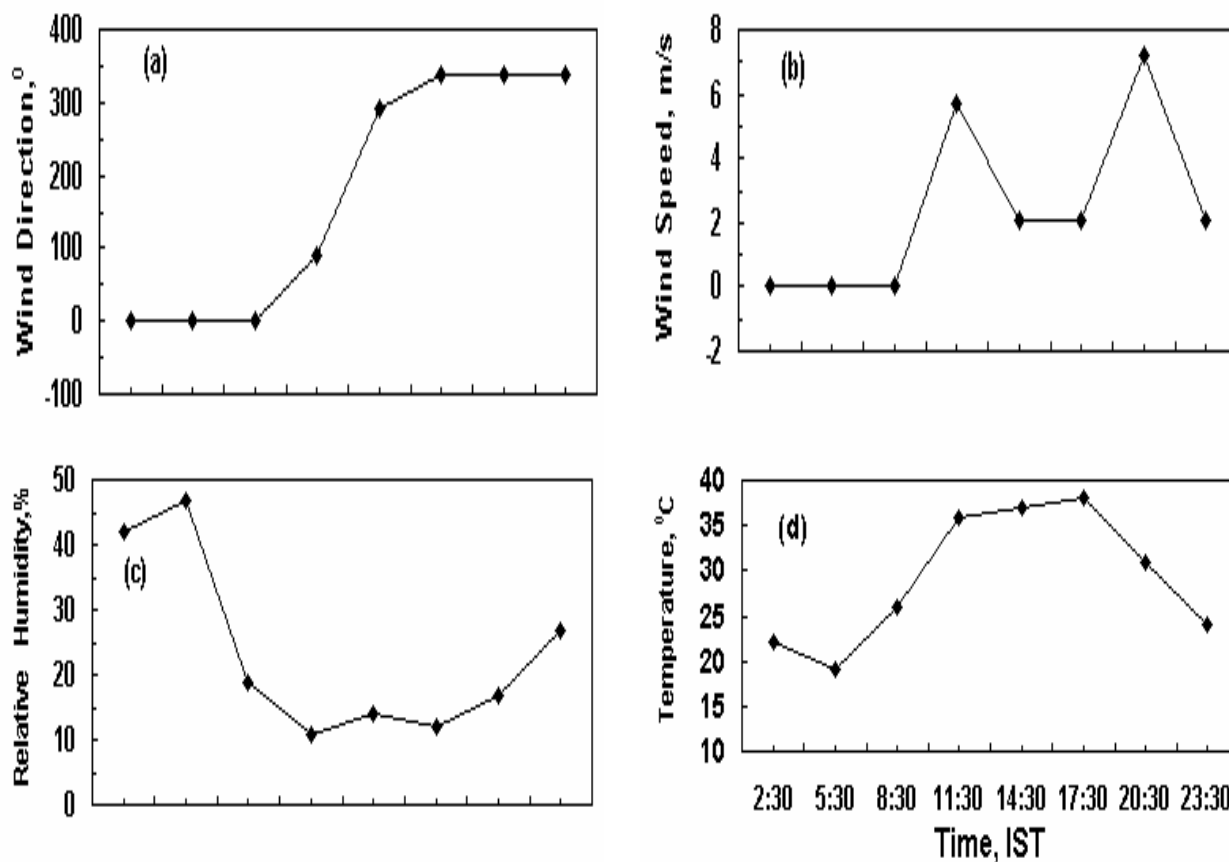
Fig. 2 (a, b, c and d). Temporal variation in meteorological parameters (wind direction, wind velocity, relative humidity & temperature).
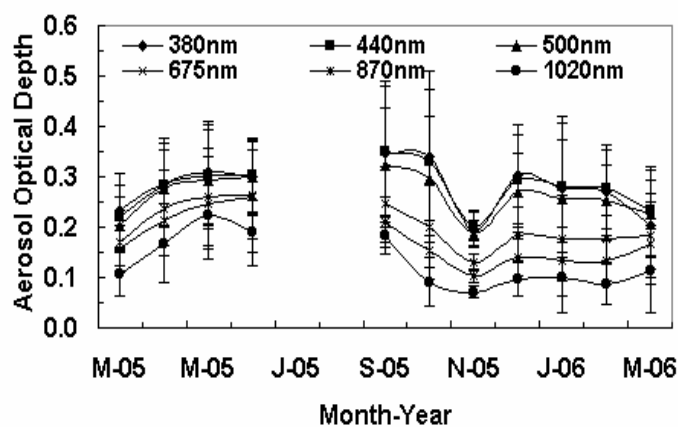
Fig. 3. Monthly variation in AOD at different wavelengths.

Monthly variation of AOD

Variation of AOD for the period March 2005 - March 2006 is shown in Fig. 3. The lowest values of mean AOD were obtained from October to December. The decrease in AOD from winter is considered to be due to cloud scavenging and rain washout processes. Monthly variation in precipitable water vapor content (PWC) is shown in Fig. 4. PWC is high in summer and low in winter, as expected. Comparison between Figs. 3 and 4 reveals a correspondence between AOD and PWC, which suggests the growth of aerosol particles associated with higher PWC values. This is in qualitative agreement with the results at other Indian stations (IMAP FINAL REPORT-III, 1994) where AOD values at all wavelengths were high in summer and low in winter.
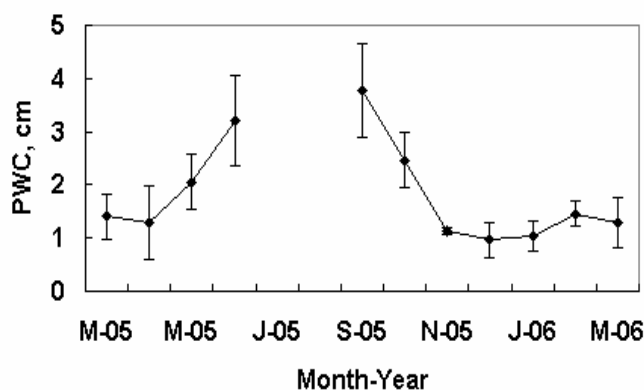
Fig. 4. Monthly variation in precipitable water vapor content.

Monthly variation of Ångström parameters, α and β

The Ångström wavelength exponent α and turbidity coefficient β have been derived from the plot of logarithm of AOD versus logarithm of wavelength. These aerosol optical and physical parameters computed for each month are plotted in Fig. 5. Our data reveal an inverse relationship between α and β values, i.e. the low exponent α values are associated with the high β values and vice-versa, which agrees with earlier observations by Adeyewa and Balogun (2003), Dani *et al.* (2003), and Satheesh *et al.* (2006). The correlation coefficient between α and β is estimated and shown in Fig. 6 to examine this feature. The correlation coefficient (R= –0.884) indicates a very good anti-correlation between α and β. Minimum values of α in summer indicate the presence of coarse-mode aerosol particles during this period, and high values of α during winter indicate the reduction of coarse-mode particles. The ratios between AOD observed at 1020 nm and at the five other wavelengths (380 nm, 440 nm, 500 nm, 675 nm, and 870 nm) are plotted in Fig. 7. This plot clearly indicates larger ratio at 380, 440 and 500 nm, implying also the abundance of coarse-

mode particles particularly during the transition period from late pre-monsoon to early monsoon months. These features indicate the presence of marine air mass, originating from the Arabian Sea, and passing over Rajkot, combined with wind-blown dust during this period. Similar results were reported by Devara *et al.* (2005) from Pune, India.
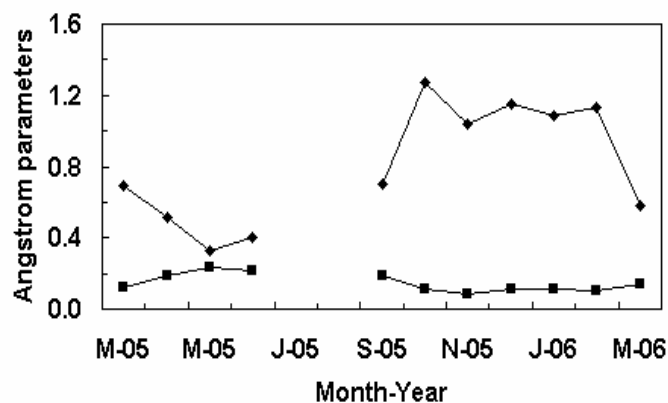

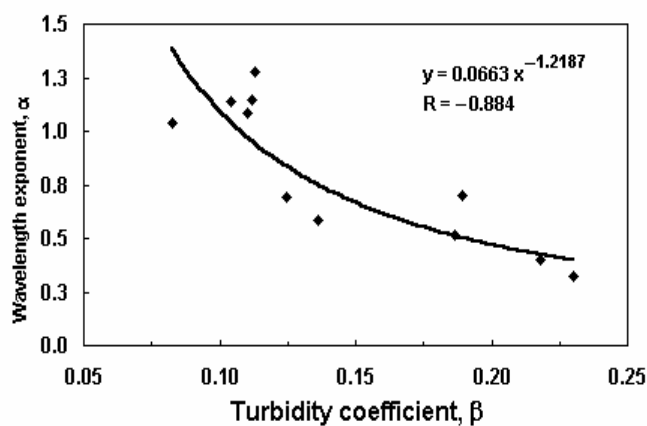**Fig. 5.** Monthly variation in Ångström parameters (wavelength exponent, α & turbidity coefficient, β).

Fig. 6. Inverse relation between wavelength exponent, α & turbidity coefficient, β.
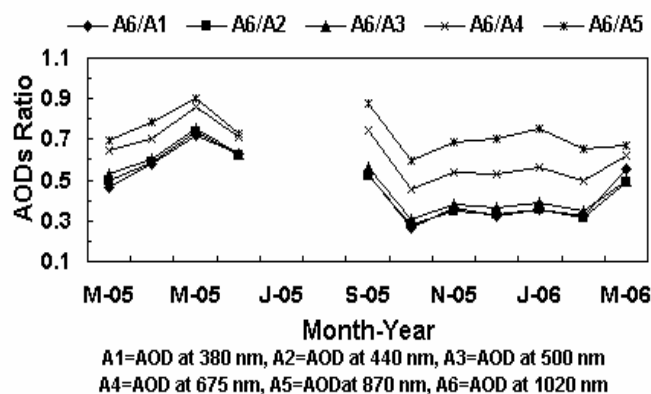
Fig. 7. Larger ratios at 380 nm, 440 nm and 500 nm, implying also the abundance of coarse-mode particles.

CONCLUSIONS

The results of the observations of optical and meteorological data for the period March 2005 to March 2006 indicate the following:

1. Spectral dependence of AOD with higher values at smaller wavelengths and vice versa. High value of AOD in summer (pre-monsoon) and low in winter (post-monsoon).
2. Smaller wavelength exponent and larger turbidity coefficient indicating abundance of coarse-mode aerosols (originating from wind-blown dust and marine airmass) particles with greater extinction during summer due to local meteorology and vice versa in winter. Sharp fall in AOD from summer to winter is considered to be due to cloud scavenging and rain washout processes.
3. There is inverse relation between wavelength exponent α and turbidity coefficient β with good anti-correlation.

ACKNOWLEDGEMENTS

REFERENCES

Adeyewa, Z.D. and Balogun, E.E. (2003). Wavelength Dependence of Aerosol Optical Depth and the Fit of the Ångström Law, *Theor. Appl. Climatol*. 74: 105-122.

Ångström, A. (1961). Techniques of Determining the Turbidity of the Atmosphere, *Tellus*. 8: 214-223.

Cachorro, V.E., de Frutos, A.M. and Casanova, J.L. (1987). Determination of the Ångström Turbidity Parameters, *App. Optics*. 26: 3069-3076.

Dani, K.K., Maheshkumar, R.S., and Devara, P.C.S. (2003). Study of Total Column Atmospheric Aerosol Optical Depth, Ozone and Precipitable Water Content Over Bay of Bengal During BOBMEX-99, *Proc. Indian Acad. Sci. (Earth Planet. Sci.)* 112: 205-221.

Devara, P.C.S., Saha, S.K., Raj, P.E., Sonbawne, S.M., Dani, K.K., Tiwari, Y.K. and Maheskumar, R.S. (2005). A Four-Year Climatology of Total Column Tropical Urban Aerosol, Ozone and Water Vapor Distributions over Pune, India. *Aerosol Air Qual. Res.* 5: 103-114.

Holben, B.N., Tanre, D., Smirnov, A., Eck, T.F., Slutsker, I., Abuhassan, N., Newcomb, W.W., Schafer, J.S., Chatenet, B., Lavenu, F., Kaufman, Y.J., Castle, J.V., Setzer, A., Markham, B., Clark, D., Frouin, R., Halthore, R., Karneti, A., O'Neil, N.T., Pietras, C., Pinker, R.T., Voss, K. and Zibordi, G. (2001). An Emerging Ground-based Aerosol Climatology: Aerosol Optical Depth from AERONET. *J. Geophys Res*. 106: 12067–12097.

IMAP FINAL REPORT-III. (1994). *Characteristics of Aerosol Spectral Optical Depths over India*, ISRO-IMP-SR-43-94. p.1-78.

Kaufman, Y.J. and Fraser, R.S. (1983). Light Extinction by Aerosols During Summer Air Pollution, *J. Clim. Appl. Meteoro*. 22: 1694-1725.

Krishnamoorthy, K., Nair Prabha, R. and Krishnamurthy, B.V. (1988). A Study on Aerosol Optical Depth at a Coastal Station, Trivandrum, *Ind. J. Radio & Space Phys*. 17: 16-22.

Maheshkumar, R.S., Devara, P.C.S., Dani, K.K. and Raj, P.E. (2001). Optical Characteristics of Aerosol as Inferred from a High Spectral Resolution Radiometer Observation over Pune During the Index ifp-99, *Current Sci*. (supplement). 80: 115-119.

Mani, A., Chacko, O. and Hariharan, S. (1969). A Study of Ångström's Turbidity Parameters from Solar Radiation Measurements in India, *Tellus*. 21: 829-843.

Morys, M., Mims, III, F. M., Hagerup, S., Anderson, S. E., Baker, A. Kia, J. and Walkup, T. (2001). Design, Calibration, and Performance of Microtops II Handheld Ozone Monitor and Sunphotomerer. *J. Geophys. Res*. 106: 14573-14582.

Pinker, R.T., Pandithurai, G., Holben, B.N., Dubovik, O. and Aro, T.O. (2001). A Dust Out Break Episode in Sub- Sahel West Africa. *J. Geophys. Res*. 106: 22,923-22,930.

Prospero, J.M., Charlson, R.J., Mohnen, B., Jaenicke, R., Delany, A.C., Mayers, J. and Rahn, K. (1983). The Atmospheric Aerosol System –An Overview, *Rev. Geophys. Space Phys*. 21:

1607-1629.

Ramanathan, V., Crutzen, P.J. and Lelievld, J. (2001). Indian Ocean Experiment: An Integrated Analysis of the Climate Forcing and Effects of the Great Indo-Asian Haze, *J. Geophys Res-Atmos*. 106: 28371-28398.

Satheesh, S.K. and Ramanathan, V. (2000). Large Differences in the Tropical Aerosol Forcing at the Top of the Atmosphere and Earth's Surface, *Nature*. 405:60-63.

Satheesh, S.K., KrishnaMoorthy, K., Kaufman, Y.J. and Takemura, T. (2006). Aerosol Optical Depth, Physical Properties and Radiative Forcing Over the Arabian Sea, *Meteorol Atmos Phys*. 91: 45-62.

Subbaraya, B.H., Jayaraman, A., Krishnamoorthy, K. and Mohan, M. (2000). Atmospheric Aerosol Studies under ISRO's Geosphere Biosphere Programme, *J. Ind. Geophys*. Union, 4: 77-90.